On optimisation of cluster-based sensor network tracking system

Yongcai Wang*

Institute for Interdisciplinary Information Sciences (IIIS),
Tsinghua University,
Beijing, 100084, China
E-mail: wangyc@tsinghua.edu.cn
*Corresponding author

Qianchuan Zhao, Dazhong Zheng and Xiaohong Guan

Center For Intelligent and Networked System (CFINS),
Department of Automation,
Tsinghua University,
Beijing, 100084, China
E-mail: zhaoqc@tsinghua.edu.cn
E-mail: dauzdz@tsinghua.edu.cn
E-mail: xhguan@tsinghua.edu.cn

Abstract: Tracking mobile targets using low-cost Wireless Sensor Network (WSN) requires not only good tracking accuracy but also network longevity. Cluster-based tracking protocols leverage the fact that only sensors in the vicinity of the target can contribute to target detection, while other sensors should sleep to save energy, which provides good tradeoff between energy efficiency and tracking accuracy. However, for the complexity of cluster-based tracking protocols, it is challenging to quantify the tradeoff between energy efficiency and tracking accuracy. In this paper, a convolution-based method is presented to quantify the relationship between the cluster parameters and the energy–quality metrics of the tracking system, which provides Pareto optimal parameters to jointly optimise the energy efficiency and the tracking accuracy of cluster-based WSN tracking system. The presented results are verified in popular cluster-based tracking protocols via extensive simulations, which shows the effectiveness of the optimisation framework.

Keywords: WSN; wireless sensor network; target tracking; cluster; optimisation; tracking performance; energy efficiency, tradeoff.

Reference to this paper should be made as follows: Wang, Y.C., Zhao, Q.C., Zheng, D.Z. and Guan, X.H. (xxxx) 'On optimisation of cluster-based sensor network tracking system', *Int. J. Ad Hoc and Ubiquitous Computing*, Vol. x, No. x, pp.xxx–xxx.

Biographical notes: Yongcai Wang is now an Assistant Researcher at Network Science group of Institute for Interdisciplinary Information Science (IIIS), Tsinghua University. He was Postdoctoral Researcher at IIIS from 2009 to 2011. Before joining IIIS, he worked as an Associate Researcher in Information Gathering and Presentation (IGP) group in NEC Labs. China from 2007 to 2009. He got my PhD and BS in 2006 and 2001 respectively, both from Department of Automation, Tsinghua University. His research interests include distributed optimisation in wireless networks, spatial and time series analysis for real-time data, mobile computing system etc.

Qianchuan Zhao received the BE Degree in Automatic Control in July 1992, the BS Degree in Applied Mathematics in July 1992, and the PhD Degree in Control Theory and its Applications in July 1996, all from Tsinghua University, Beijing, China. He is currently a Professor and the Associate Director of the Center for Intelligent and Networked Systems (CFINS), Department of Automation, Tsinghua University, Beijing, China. He was a Visiting Scholar at Carnegie Mellon University and Harvard University in 2000 and 2002, respectively. His research interests include discrete event dynamic systems (DEDS) theory and applications, optimisation of complex systems, and wireless sensor networks.

Dazhong Zheng received the diploma in automatic control from Tsinghua University, Beijing, China, in 1959. Since 1959, he has been with the Department of Automatic Control, Tsinghua University, where he is a Professor in Control Theory and Engineering. He was a Visiting Scholar in Department of Electrical Engineering, State University of New York at Stony Brook,

from 1981 to 1983 and in 1993. His research interests include linear systems, discrete event dynamic systems, and power systems. He has published many journal papers and five books. He is Vice Chairman of the Control Theory Technical Committee for Chinese Association of Automation (CAA) and a Deputy Editor-in-Chief of Acta Automatica Sinica, Beijing, China.

Xiaohong Guan received the BS and MS Degrees in Automatic Control from Tsinghua University, Beijing, China, in 1982 and 1985, respectively, and the PhD Degree in Electrical Engineering from the University of Connecticut, Storrs, in 1993. He was a Senior Consulting Engineer with PG&E from 1993 to 1995. From 1985 to 1988, and since 1995, he has been with the Systems Engineering Institute, Xian Jiaotong University, Xian, China, and currently, he is the Cheung Kong Professor of Systems Engineering, the Dean of School Electronic and Information Engineering, and Director of the Systems Engineering Institute. He is also the Director of the Center for Intelligent and Networked Systems and served as Head of the Department of Automation, Tsinghua University, from 2003 to 2008.

This paper is a revised and expanded version of a paper entitled 'Clusters partition and sensors configuration of target tracking in wireless sensor networks' presented at *ICESS2004*, Hangzhou, China, December, 2004.

1 Introduction

Wireless Sensor Network (WSN) composed of network of distributed smart microsensors is rapidly emerging in recent years as a feasible solution to a wide range of applications. Among these applications, mobile target tracking is the most promising one, which can be widely applied in livestock farming, wildlife monitoring, battlefield surveillance, etc.

A typical application scenario of the WSN tracking system is to deploy a large amount of micro sensors in the Area-of-Interest (AOI) to track the mobile targets, such as livestock tracking in the farmland, enemy tracking in the battle field, etc. The targets' positions are estimated by the spatially distributed monitoring sensors using range-based or range-free localisation techniques. Such target tracking systems pose fundamental requirements for energy efficiency and tracking accuracy.

- Since the microsensors are commonly battery powered and are difficult to recharge after deployment, conserving node energy is the primary requirement. Letting sensors work in duty cycling mode is the major technique for sensor energy conservation (Demirbas et al., 2006; Sharp et al., 2005; Wang et al., 2010), but the sensor is dis-functional in 'sleep' mode, which cannot track the targets. This leaves great challenge for sensor scheduling.
- High-tracking accuracy is always the requirement of a tracking system, which generally requires more sensors to contribute to the target detection and position calculation. It basically contradicts with the energy conservation requirement of the sensor network.

To address these two requirements, cluster-based target tracking protocols were proposed as promising solutions. They leverage on the fact that the tracking quality is only determined by the sensors that are in the vicinity of the target, while faraway sensors that cannot detect the target should sleep to save energy. Therefore, the networked sensors are organised into clusters based on their spatial information. When a target is approaching a cluster, sensors in this cluster switch to active mode to track the target, while sensors in other clusters can sleep to save energy. To avoid missing target, sleeping sensors are pre-activated based on the predicted moving direction of the target. Further, the sensors in the active cluster will switch to sleep model after the target leave their sensing regions.

Cluster-based target tracking provides good tradeoff between the energy efficiency and the tracking quality. But it also introduces complex cluster partition, sensor activation and deactivation functionalities, etc. These complex sensor network functions make the quantitative analysis to the energy and tracking accuracy performances very difficult. Heuristics and simulations are currently main solutions for the design and evaluation of the cluster-based tracking protocols. How to optimise the cluster-based tracking system remains as a big challenging problem.

This paper proposes a novel convolution method to quantify the relationship between the clustering parameters and the energy–tracking accuracy performances of the tracking system. The energy consumption rate and the tracking accuracy are derived as functions of the cluster size, node density, sensing radius, the activation mechanism, etc. The relationship is further utilised to optimise the design of the cluster-based tracking system, which provides Pareto optimal parameters to jointly optimise the energy efficiency and the tracking accuracy.

The practical effectiveness of the relationship is verified in an extensive manner in popular cluster-based tracking protocols. In these verifications, realistic conditions such as non-uniform sensor deployment, cluster irregularity and the target randomness are considered. The results show that the relationship can well predict the tracking performances in various network scenarios and it can be rather confidently adopted as a design guideline for optimising the cluster-based tracking system.

The remainder of this paper is organised as follows. The cluster parameters and the energy–quality metrics are introduced in Section 2. The relationship derivation and

Pareto optimisation framework are presented in Section 3. Verifications in popular cluster-based tracking protocols are presented in Section 4. The related work is introduced in Section 5 and the paper is concluded in Section 6.

2 Assumptions and cluster parameters

2.1 System model

A cluster-based target tracking system can be characterised by a set of parameters. Although it is difficult to characterise all the clustering, target movement and environment dynamics, some essential behaviours can be quantified.

- Let us consider the AOI is a 2D field, denoted by S. N sensors are uniformly deployed in it with density $\rho = N/S$. The positions of these sensors are denoted by $\mathbf{X} = \{x_i, y_i, i = 1, \ldots, N\}$.
- Sensors' communication radius is denoted by r and sensing radius is denoted by s.
- The sensors are assumed organised into n clusters, according to their spatial relations. Each cluster covers a circular area with radius c, centred at a point $\boldsymbol{h}_j = \{x_j^h, y_j^h\}$, where j is the index of the cluster. Sensors located in the circular cluster area belong to the corresponding cluster and are managed by an elected head of the cluster.
- The target moves along some unknown trajectory in the AOI. Its position at time t is denoted by $\theta_t = (\theta_{x,t}, \theta_{y,t})$.
- To track target while saving energy, clusters are activated and deactivated to track the target. We assume that an activated/deactivated cluster will activate/deactivate all the sensors in this cluster. A sensor can detect the target only if it is active and the target is in its sensing range.

2.2 Parameters to characterise the cluster-based tracking scenario

The above model is general, which is capable of describing almost all the cluster-based tracking protocols. The shapes of the sensing region and the clusters are not restricted to be circles, but can be extended to other irregular shapes.

Proposition 1: *The temporal behaviour of the cluster-based tracking system at time* t *can be characterised by a set of parameters:* $\{r, c, s, \rho, N, n, \boldsymbol{\theta}_t\mathbf{A}_t, \mathbf{H} = \{h_1, h_2, \ldots, h_n\}, \mathbf{X}\}$, *where* A_t *stands for the states of the sensors, i.e., if the ith sensor is active at time t,* $A_t(i) = 1$, *otherwise,* $A_t(i) = 0$. *H stands for the centres of the cluster areas and X stands for the positions of the sensors. This set of parameters is called parameters of the cluster-based tracking system.*

Proof of Proposition 1 is straightforward. **H** determines the positions of the cluster areas; c determines the radius of cluster areas, so that the n disc-shaped cluster areas are uniquely determined in the two-dimensional region. As the positions of these N sensors are also known, to which cluster a sensor belongs is determined by $\{\mathbf{H}, \mathbf{X}, c\}$. Besides this, the states of all sensors can be referred to vector **A**, and whether a sensor can detect the target is determined by the condition $\|\mathbf{x} - \boldsymbol{\theta}_t\| \le s$, where **x** stands for the coordinates of this sensor. Therefore, from $\{\mathbf{H}, \mathbf{X}, c, \mathbf{A}, s, \boldsymbol{\theta}_t, n, N\}$, we know the distributions of the cluster and we also know which sensor is active and which sensor can detect the target. □

In the next section, we will further show that the system performance is mainly determined by parameters $\{r, c, s, \rho, n, N\}$.

3 Relationship between cluster and system performances

3.1 The tracking quality performance

Figure 1 shows an instance of the cluster-based tracking scenario. An active cluster is shown by a dashed circular radius c. The target-detectable area is a circular area centred at the target with radius s.

Figure 1 Cluster-based target tracking scenario. The circular area C_a is the active cluster area. Sensors in this area are active and sensors outside this area are sleeping. D is the target detectable area. Only the sensors in the overlapping area of D and C_a are both active and within the sensing range of the target. We call the sensors in the overlapping area the contributable sensors (see online version for colours)

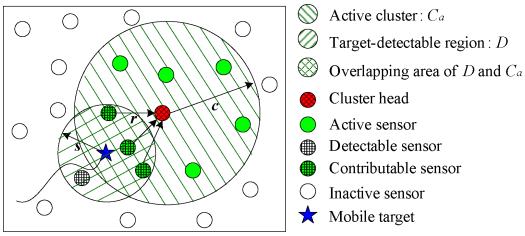

Note that only the sensors located in the overlapping area of these two circles can contribute to the target tracking. We call these sensors ***contributable sensors*** which are denoted by n_s. Clearly, the number of contributable sensors has an important impact on the target tracking accuracy. This impact is examined in various target detection techniques. The popular target detection techniques can be categorised into two classes.

- Sensors can measure the distance to the target and infer the location of target by geometry-based methods (Priyantha et al., 2000).
- Sensor only detects the appearance of the target. It is a binary detection. Centroid method (Aslam et al., 2003) etc. are needed to estimate the target's position.

These two methods differ greatly in hardware, etc. However, they are common in the principle for achieving

accurate target detection: *the more the better*. The more sensors contribute to the target detection, the more accurate the target tracking is.

Based on such an observation, the tracking quality metric can be extracted as the expected number of the contributable sensors, $Q = E\{n_s\}$. It is obvious that n_s is determined by the expected overlapped area of the target-detectable area and the active cluster area. We denote this overlapping area as S_d. Therefore, *the quality metric* can be described as:

$$Q = E(n_s) = \rho E(S_d). \tag{1}$$

The validity of this quality metric is easily understood from the estimation theory. The standard derivation (confidence interval) of the estimation is of the order of magnitude $O(\sqrt{n})$, where n is the number of contributable sensors in this problem. We formulate this statement as a Theorem.

Theorem 1: *If the observations of the sensors are independent with each other and the measurement noise is irrelevant with the distance between the sensor and the target, then the standard derivation of the positioning accuracy converges at* $O(1/\sqrt{n_s})$, *where* n_s *is the number of the contributable sensors.*

Proof: Theorem 1 can be proved by analysing the magnitude of the standard derivation for the different detection techniques. Details of the proof for different location detection techniques are given in the Appendix. A remark is that in the second category, the way to increase the tracking accuracy is to increase the nodes density. Because the minimum expected error is dominated by the inter-node distance in this kind of detection technique.

3.2 Convolution method to formulate the quality metric

Note that the expected number of the contributable sensors is determined by the overlapping area of two circles, i.e., the active cluster and the circle centred at the target with radius s, respectively. Therefore, convolution-based method can be utilised to evaluate the quality metric. If we denote x as the distance from the centre of the active cluster area to the position of the target, the overlapped area S_d will be a function of x, and the expression of $S_d(x)$ can be derived.

$$S_d(x) = 2\int_{-\infty}^{+\infty} \sqrt{c^2 - \tau^2}\sqrt{s^2 - (x-\tau)^2}\, \mathrm{d}\tau. \tag{2}$$

Figure 2 uses two half circles to show how convolution works on the two circular areas. The expression of $S_d(x)$ can be calculated as a piece-wise function:

$$\begin{cases} S_d(x) = \pi s^2 & \text{when } c - s > x > s - c \\ S_d(x) = -f_s(y) & \\ \quad -f_c(z) + \dfrac{\pi(s^2 + c^2)}{4} & \text{when } c + s > x > c - s \\ S_d(x) = 0 & \text{otherwise} \end{cases}, \tag{3}$$

where

$$f_s(y) = \left(\frac{y}{2}\sqrt{s^2 - y^2} + \frac{s^2}{2}\arcsin\frac{y}{s}\right),$$

$$f_c(z) = \left(\frac{z}{2}\sqrt{c^2 - z^2} + \frac{R^2}{2}\arcsin\frac{z}{c}\right).$$

$$y = \frac{s^2 - c^2 + x^2}{2x} \text{ and } z = \frac{c^2 - s^2 + x^2}{2x}$$

are used to simplify the expression. We can see the result is complex for further use in optimisation. But it can be well approximated by another piece-wise linear function $\tilde{S}_d(x)$ (shown in the dashed lines in Figure 3):

$$\begin{cases} \tilde{S}_d(x) = \pi s^2 & \text{when } c - s > x > s - c \\ \tilde{S}_d(x) = -\dfrac{1}{2}\pi s(x - c - s) & \text{when } c + s > x > c - s \\ \tilde{S}_d(x) = 0, & \text{otherwise} \end{cases}. \tag{4}$$

$\tilde{S}_d(x)$ is much simpler, which will greatly simplify the derivation of the relationship and further optimisation. Before accepting $\tilde{S}_d(x)$, we compare $S_d(x)$ and $\tilde{S}_d(x)$ for different s and c to check how $\tilde{S}_d(x)$ approximates $S_d(x)$. We normalise s to 1 and vary c and x to calculate the bound of $S_d(x) - \tilde{S}_d(x)$. More specifically, we denote three functions in the error analysis.

$$\text{delta}_1(c) = \max_x(S_d(c) - \tilde{S}_d(c)) \tag{5}$$

$$\text{delta}_2(c) = \min_x(S_d(c) - \tilde{S}_d(c)) \tag{6}$$

$$\text{delta}_3(c) = \text{delta}_1(c) - \text{delta}_2(c). \tag{7}$$

Figure 2 Illustration of the convolution method

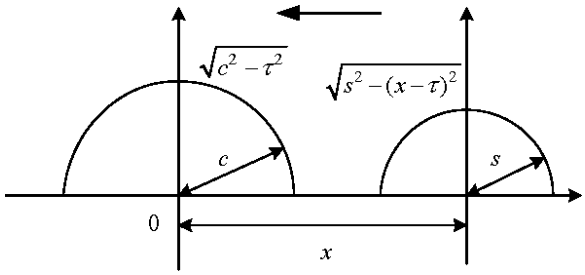

Figure 3 The function curve of $S_d(x)$ (see online version for colours)

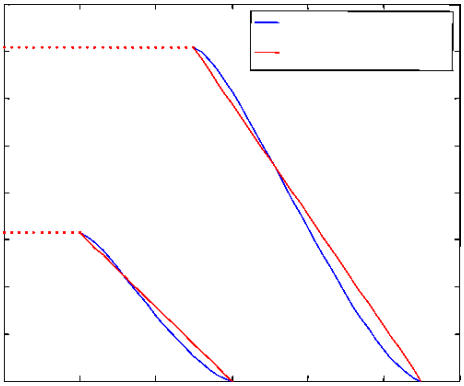

The results of $\text{delta}_1(c)$, $\text{delta}_2(c)$ and $\text{delta}_3(c)$ are plotted in Figure 4. They show that for different parameter settings of c, s and x, the difference between the upper bound and the lower bound of the approximation error is bounded and very small. So we are confident to use $\tilde{S}_d(x)$ to represent the overlapping area in the following analysis. Therefore, the expected quality metric can be formulated as:

$$Q = E\{n_s\} = E\{\rho S_d\} = \rho E(\tilde{S}_d) = \rho \int_0^{c+s} f(x)\tilde{S}_d(x)\,\mathrm{d}x, \quad (8)$$

where $f(x)$ is the *pdf* (probability density function) of x. To present the relationship theoretically, we discuss two kinds of distributions of $f(x)$: uniform and normal. Later in Section 6.3, we will show that the relationships are robust to the different hypothesis of $f(x)$, which is due to the monotone structure of the performance metrics.

Figure 4 Error analysis of $S_d(x)$ and $\tilde{S}_d(x)$ (see online version for colours)

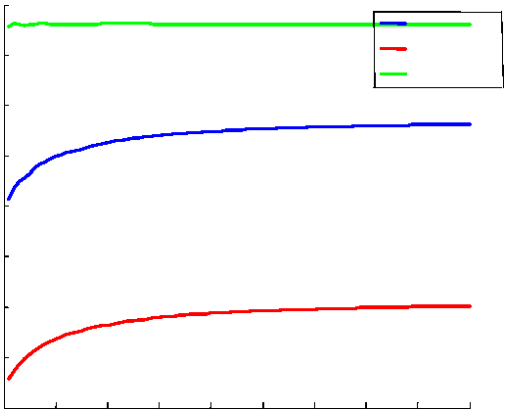

An assumption of $f(x)$ is that x follows normal distribution with parameters (μ, σ). This means that the target has higher probability to appear at a normal distance to the cluster centre than appear too close or too far. We set $\mu = (c + s)/2$ and $\sigma = (c + s)/6$ so that the probability that $0 \le x \le c + s$ is equal to $P(\mu - 3\sigma \le x \le \mu + 3\sigma) = 99.73\%$. Expression of $E(\tilde{S}_d)$ can be derived as:

$$\begin{aligned} E(\tilde{S}_d) = \frac{1}{C}\Bigg\{ & \frac{1}{2}\sqrt{\frac{\pi}{2}}s\sigma\left[\exp\left(-\frac{(c+s-\mu)^2}{2\sigma^2}\right)\right. \\ & \left.-\exp\left(-\frac{(c-s-\mu)^2}{2\sigma^2}\right)\right] + \frac{1}{2}\pi s^2 \operatorname{erf}\left(\frac{\mu}{\sqrt{2}\sigma}\right) \\ & -\frac{1}{4}\pi s(c-s-\mu)\operatorname{erf}\left(\frac{c-s-\mu}{\sqrt{2}\sigma}\right) \\ & +\frac{1}{4}\pi s(c+s-\mu)\operatorname{erf}\left(\frac{c+s-\mu}{\sqrt{2}\sigma}\right)\Bigg\} \end{aligned} \quad (9)$$

where

$$C = \int_0^{\infty} \frac{1}{\sqrt{2\pi\sigma^2}} \exp\left(-\frac{(x-\mu)^2}{2\sigma^2}\right)\mathrm{d}x = \frac{1}{2} + \frac{1}{2}\operatorname{erf}\left(\frac{\mu}{\sqrt{2}\sigma}\right)$$

is a normalisation constant, and

$$\operatorname{erf}(x) = \frac{2}{\sqrt{\pi}}\int_0^x \exp(-t^2)\,\mathrm{d}t$$

is the 'error function' encountered in the integration of the normal distribution (Medeiros et al., 2008).

Another reasonable assumption of $f(x)$ is that x is uniformly distributed in the close set $[0, c + s]$. This means that the target has the same probability to appear any close or any far from the cluster centre within the range $[0, c + s]$. In this case, $E(\tilde{S}_d) = \pi c s^2/(c + s)$. So that, we have formulated how the cluster scheme will affect the tracking quality performance. Now let us consider how it affects the energy performance.

3.3 The energy metric

Sensors sense target generally in discrete time. Therefore, we define an energy-metric as the energy consumption of sensors for one target detection. The metric is built based on the energy models in Sharp et al. (2005), Wang et al. (2010), Wang et al. (2006), He et al. (2006) and Wang et al. (2004). Sensors consume energy mainly according to four kinds of operations: packet transmitting, packet receiving, sensing and data processing. It was shown in Heinzelman et al (2000) and Wang et al. (2004), if a sender transmits a k bytes packet, the energy consumed by it is $T_x = E_{\text{elec}}k + \varepsilon_{\text{amp}}kd^{\alpha}$, where $E_{\text{elec}}(nJ/\text{bit})$ and $E_{\text{amp}}(pJ/\text{bit}/m^{\alpha})$ are the energy coefficients of the radio circuit and the amplifier; $\alpha \in [2, 4]$ is the path loss exponent; d is transmission distance. The energy consumed by the receiver is independent of the distance, which is modelled as $R = E_{\text{elec}}k$. Energy for sensing is modelled in Sharp et al. (2005) as: $S = E_{\text{sensor}}s^2$, where s is the sensing radius and E_{sensor} is the energy coefficient of the sensor. Energy dissipation for data processing is assumed proportional to the packet length $F = E_{\text{cpu}}k$, where E_{cpu} is the energy coefficient of the processor.

The energy consumption is also affected by the working states of the sensors. Considering a target tracking instance, the energy consumption of the sleeping sensors can be omitted. The sensors in the active cluster are in sensing mode. Their energy consumption for sensing target is $S \cdot n_c = E_{\text{sensor}}s^2\ \pi c^2\rho$. Only the sensors in the overlapped area of the active cluster and the target-detectable region can actually detect the target. They will send the detected information to the cluster head. The energy consumption for the packet transmission is $T_r \cdot n_s = (E_{\text{elec}}k + \varepsilon_{\text{amp}}kr^{\alpha}) \cdot S_d\rho$. These n_s packets will be received by the cluster head. The energy consumption by the receiving operations is $R \cdot n_s = (E_{\text{elec}}k) \cdot S_d\rho$. Then, these packets will be processed by the cluster head, with additional energy consumption for data processing $F \cdot n_s = (E_{\text{cpu}}k) \cdot S_d\rho$. At last, the processed result will be sent to the base station by the cluster head with a larger communication radius, which is commonly set as c. So the transmission energy consumed by the cluster head is $T_c = (E_{\text{elec}}k + \varepsilon_{\text{amp}}kc^{\alpha})$. Without loss of generality, we assume $k = 1$, so the total energy consumption for one target detection can be formulised as:

$$E = Sn_c + T_r n_s + Rn_s + Fn_s + T_c$$
$$= E_{\text{sensor}} s^2 \pi c^2 \rho + S_d \rho (E_{\text{elec}} + E_{\text{cpu}} + E_{\text{elec}} + \varepsilon_{\text{amp}} r^{\alpha}) + E_{\text{elec}} + \varepsilon_{\text{amp}} c^{\alpha}. \quad (10)$$

3.4 Energy–quality tradeoffs

Based on the quality and energy performance metrics of equations (9) and (10), the underlying relationships between cluster parameters and system performances can be characterised. Looking into the relationship will help us to find the key parameters that affect the energy–quality tradeoff in cluster-based target tracking.

It is easy to see that the parameter $\{r\}$ appears only in the energy metric, while the parameters $\{s, c, \rho\}$ appear in both the energy and the quality metrics. Relations (9) and (10) are both monotone linear increasing functions of ρ, so the energy and the quality metrics are indeed dominated by the parameter set $\{s, c\}$, i.e., the sensing radius and the cluster radius. But in the real applications, the cluster radius c is commonly not a decision variable. Instead, it is determined by the number of the partitioned clusters (n) with the constraint that the AOI is fully covered by the cluster areas. As the coverage area of n clusters is $n\pi c^2$, applications commonly require $n\pi c^2/S = O_r$, where $O_r \geq 1$ is the cluster coverage rate. n is the decision variable and c is determined by $c = \sqrt{O_r S / n\pi}$. So the energy–quality metrics are indeed dominated by the parameters $\{n, s\}$. We use the parameter settings in Table 1 to visually show how the energy and quality metrics are affected by $\{n, s\}$. For saving space, we only choose equations (9) and (10) that are derived by the normally distributed $f(x)$ to show the properties. The results are shown in Figures 5 and 6.

Table 1 Parameter settings for visualisation of energy–quality tradeoff

	Value	*Meaning*
E_{ini}	10 J	Initial energy of sensor nodes
E_{elec}	5.0e-9	Circuitry coefficient
E_{cpu}	1.0e-8	CPU coefficient
ρ	0.1	Sensor density
α	3	Pass loss exponent
Q_r	$\pi/2$	Cluster coverage rate
E_{sensor}	1.0e-10	Sensing coefficient
E_{amp}	1.0e-10	Amplifier coefficient
k	1	Data packet size
r	10 m	Communication radius
N	1000	Number of sensors

The range of s is [0, 20] and the range of n is [1, 49] in these two figures. The result shows that both the energy consumption rate (E) and the tracking quality (Q) are increasing functions of the sensing radius (s) and are decreasing functions of the number of clusters (n). This agrees with our general knowledge. The tracking quality will be better if the cluster and the sensing radius are larger, but larger cluster and larger sensing radius will consume more energy. Minimising the energy consumption contradicts with the requirement of maximising the tracking quality. This supports the widely adopted tradeoff design of the cluster-based tracking protocols (Wang et al., 2004; Chen et al., 2004). Therefore, there is no global optimal design of n and s. But equations (9) and (10) can help to select proper n and s, which can be accomplished by a Pareto optimisation method.

Figure 5 How n and s affect the energy metric (see online version for colours)

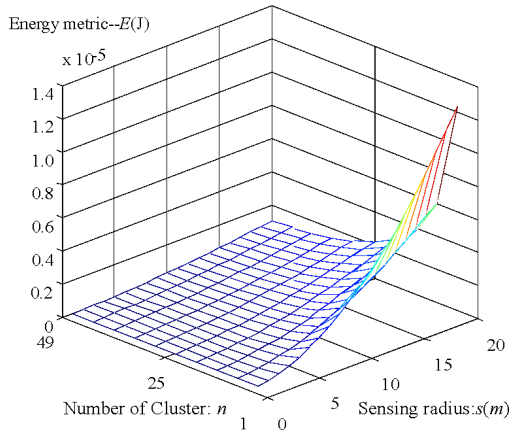

Figure 6 How n and s affect the quality metric (see online version for colours)

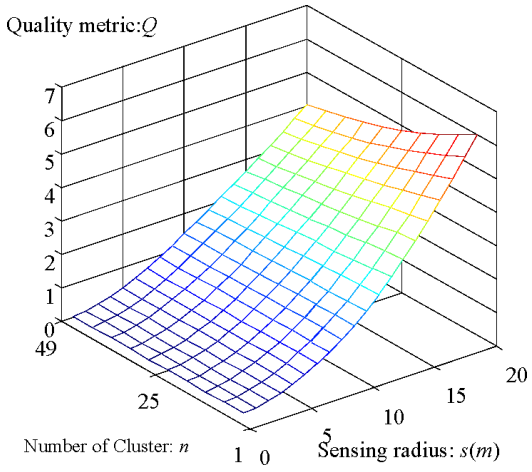

3.5 Pareto optimisation

Pareto optimality is widely applied in multiple objects multiple variables optimisation problem for discrete design space. Each design is a combination of several discrete variables. A design can be considered Pareto optimal if there is no other design that performs at least as well on every metric and strictly better on at least one metric.

To visualise the energy–quality tradeoff in Pareto optimisation, the quality metric is converted to $-Q$ to work as the x-axis; the energy metric works as the y-axis. Every design is a combination of $\{n, s\}$, which is plotted as a point in the scatter-plot with coordinates $\{-Q, E\}$. The scatter-plot results for the design space of $s \in [0, 20]$ and $n \in [1, 49]$ are

shown in Figure 7. The Pareto-optimal solutions are the points in the scatter-plot with no other points better than them in both metrics, i.e., no other points are below and left to them in the figure. We call the Pareto-optimal solutions Pareto Fronts.

In Figure 7, all the Pareto Fronts are highlighted with red circles. If an application preference is given, we only need to search among the Pareto Fronts to optimise the cluster design. An example is shown in Figure 8. The application requires at least five nodes can detect the target while reducing the energy consumption as much as possible. The optimal (n, s) design is displayed with a star. For the small searching space of the Pareto Fronts, the optimal (n, s) pair can be found within millisecond. Therefore, the derived relationship can not only predict the system performances, but also be used to optimise the system design.

Figure 7 Pareto Frontier graph of optimisation model. Each dot in the figure is a $(n.s)$ design. Its coordinates in the graph is given by its quality and energy metrics (–Q, E) (see online version for colours)

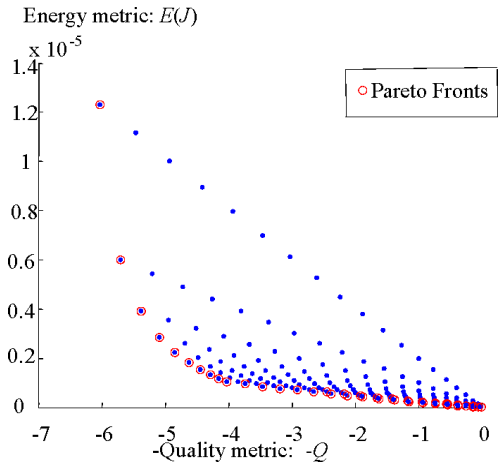

Figure 8 Pareto optimisation with application preference. The optimal solution (red star) is selected among the Pareto Fronts (dot with red circles) based on the application requirements (green line) (see online version for colours)

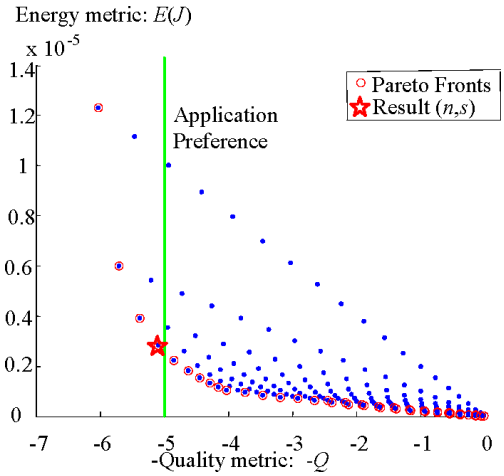

4 Evaluation in popular cluster-based tracking protocols

The effectiveness of the relationship is evaluated in popular cluster-based tracking protocols. One of the popular cluster-based target tracking is the overlapping cluster-based tracking (OCT) protocol. In the OCT protocol, cluster head is generated by 'Grid Uniform' algorithm; overlapped clusters are partitioned to cover the whole AOI and cluster is activated predictively. The performances of the OCT protocol for different cluster parameters are evaluated to verify the derived relationship.

4.1 'Grid Uniform' cluster head generation

The OCT protocol uses fully distributed 'Grid Uniform' cluster head generation algorithm. The idea is that the sensor field is divided into n equal-size imaginary grids, where n is the number of the desired clusters. Each grid has a 'Virtual Centre', which is the geometrical centre of the grid. For sensors in each grid, a distributed algorithm is run by them to elect the one closest to the 'Virtual Centre' as the cluster head. As the 'Virtual Centres' are evenly distributed in the field, the generated cluster heads are expected to be evenly distributed. The idea of grid uniform cluster head generation is shown in Figure 9.

Figure 9 'Grid Uniform' cluster head generation. '+' is the virtual grid centre. The red circle is the generated cluster head (see online version for colours)

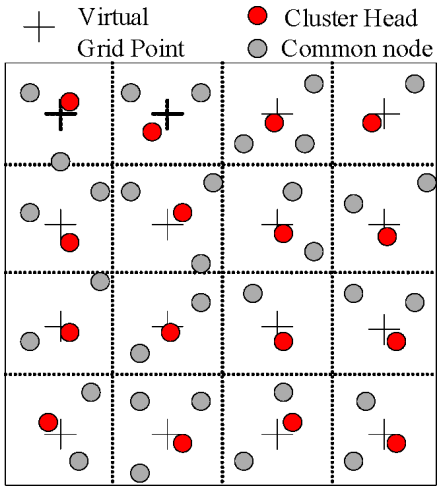

4.2 Overlapped circular shape cluster partition

After cluster head election, the OCT protocol partitions the clusters by allowing cluster overlapping. The idea is illustrated in Figure 10. Each cluster area is a circular area, centred at the generated cluster head, and with cluster radius c. Such overlapped cluster can be formed by the fully distributed method with localised communication. Each cluster head broadcasts cluster partition command with communication radius c and then turns to listen. If it receives a Reply message, it adds the sender to its

member list. Common sensors listen to the channel. If it hears a partition command, it adds the sender to its CH list and sends a Reply message. For communication collision avoidance, cluster heads and member nodes can use Collision Avoidance Multiple Access (CSMA) to broadcast partition command and Reply message. After such a cluster partition process, a sensor may join into multiple clusters. We call such kind clusters 'overlapping clusters'. Overlapping clusters partition has two main advantages.

- The number of sensors in a cluster become predictable with expected value $nc = \rho\pi c^2$. The cluster size can be controlled by adjusting the cluster radius c.
- Full coverage of the sensor field by the n clusters can be guaranteed, which can well approach the assumption that the target can always be tracked by an active cluster.

Figure 10 'Overlapping' cluster partition. Cluster head broadcast message to form 'overlapping clusters'. Sensors in overlapping areas belong to multiple clusters (see online version for colours)

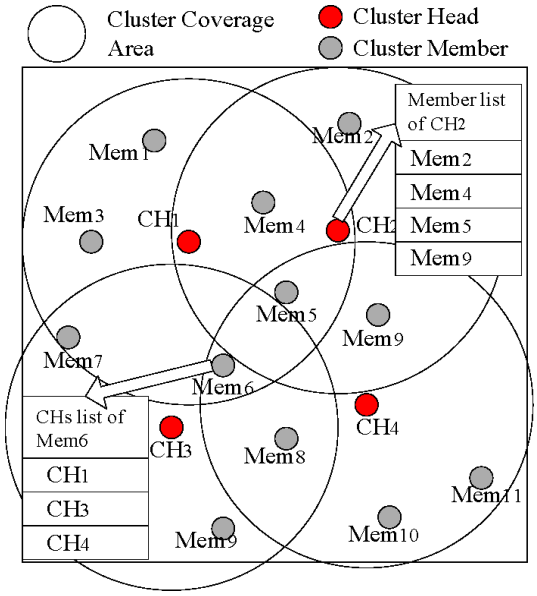

4.3 Predictive cluster switch

The OCT protocol uses predictive activation to switch clusters. Suppose the location of the target is (x_{i-1}, y_{i-1}) at time T_{i-1}, and is (x_i, y_i) at time T_i. The position of the target at time T_{i+1} is predicted to be

$$(x_i + 1, y_i + 1)\begin{cases} x_{i+1} = x_i + vt\cos(\theta) \\ y_{i+1} = y_i + vt\sin(\theta) \end{cases},$$

$$v = \frac{\sqrt{(x_i - x_{i-1})^2 + (y_i - y_{i-1})^2}}{t_i - t_{i-1}},$$

$$\theta = \cos^{-1}\frac{x_i - x_{i-1}}{\sqrt{(x_i - x_{i-1})^2 + (y_i - y_{i-1})^2}}$$

by the current cluster head CH_c with a linear predictor. Then, the cluster head sends a message to the downstream cluster head CH_d towards which the target is headed to tell the predicted target location. Suppose the location of CH_c is (x_c, y_c) and location of the CH_d is (x_d, y_d). The condition to trigger the cluster switch is that:

$$\|x_d - x_{i+1}\| + \|y_d - y_{i+1}\| < \|x_c - x_{i+1}\| + \|y_c - y_{i+1}\|. \quad (14)$$

If the condition is satisfied, the current cluster is deactivated and the downstream cluster is activated. CH_c broadcasts 'sleep' message and CH_d broadcasts 'awake' message. This switch process is different from the traditional switch schemes that the sensors in the overlapping area of CH_c and CH_d will keep active during the cluster switch. In Section 5.4, we will see this point helps much in reducing the target loss probability compared with the non-overlapped cluster partition.

4.4 Performance evaluation of the OCT protocol regarding different cluster parameters

Performances of the OCT protocol are evaluated regarding different cluster parameters. We simulated a scenario where a target moves randomly within the 200×200 (m^2), two-dimensional sensor field. N sensors are uniformly deployed in it and they are partitioned into n overlapping clusters. The simulation program is a discrete-event simulator developed using Matlab 6.5.

We firstly evaluate how the analytical relationship predicts the quality and energy performances of the OCT protocol. When $N = 1000$, 100 replications of simulation were run for every pair of (n, s) to statistically evaluate the energy metric and the quality metric of the OCT protocol. The average value of simulated energy and quality performances for all $(n.s)$ designs are shown in Figure 11(a) and Figure 11(b) in the lighter surface. The energy and quality metrics are also predicted by the derived relationship, which are plotted in the darker surfaces to compare with the simulated results.

We can see that the analytical surfaces coincide well with the simulated surfaces. The simulated surfaces are not smooth for the randomness of sensors' deployment and the randomness of the target's movement. We further define a Pareto Fronts-based metric quantitatively to check whether the Pareto Fronts derived from equations (9) and (10) are still Pareto Fronts in the simulation results.

A set of Pareto Fronts can be obtained from the analytical relationship, i.e., from equations (9) and (10). After evaluating the simulation performances, we can check whether the performances of the Pareto Fronts are still Pareto optimal in the OCT protocol. *The percent of the coincident Pareto Fronts, i.e. percent of the analytical Pareto Fronts that are still Pareto optimal in the simulations is used as a criterion***.** The result is shown in Figure 11(c). The analytical Pareto Fronts are indicated by the red circles, and their performances in the OCT protocol are indicated by their coordinates. Statistical measurement

shows that 91.4% analytical Pareto Fronts are still Pareto optimal. This indicates that equations (9) and (10) can be effectively used as a design guideline for the selection of the cluster parameters.

When $N = 200$, these verification results are shown in Figure 12. The relationship between the energy–quality metrics and the cluster parameters is also effectively predicted by equations (9) and (10) as shown in Figure 12(a) and (b). The percent of the coincident Pareto Fronts is measured as 90.7% as shown in Figure 12(c). More verification was done for more network settings and different target patterns. In these experiments, the relationship derived with the uniformly hypothesised $f(x)$ is also considered. The results are summarised in Table 2. The coincident rate of the Pareto Fronts is larger than 75% for the worst case when the target moves in a random walk. Relationships derived with normal hypothesis and uniform hypothesis provide similar results. The results show that the derived relationship can work as an important design guideline for the OCT protocol.

Figure 11 Relationship verification when $N = 1000$: (a) energy metric; (b) quality metric and (c) How the Pareto Fronts derived from the relationship perform in the simulation (see online version for colours)

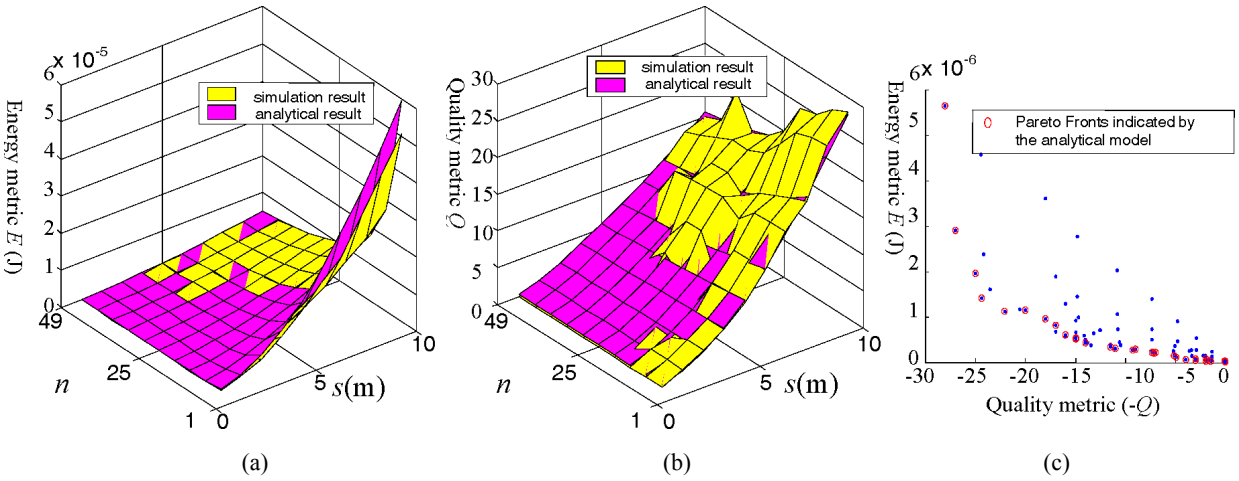

Figure 12 Relationship verification when $N = 200$: (a) energy metric; (b) quality metric and (c) how the Pareto Fronts derived from the relationship perform in the simulation (see online version for colours)

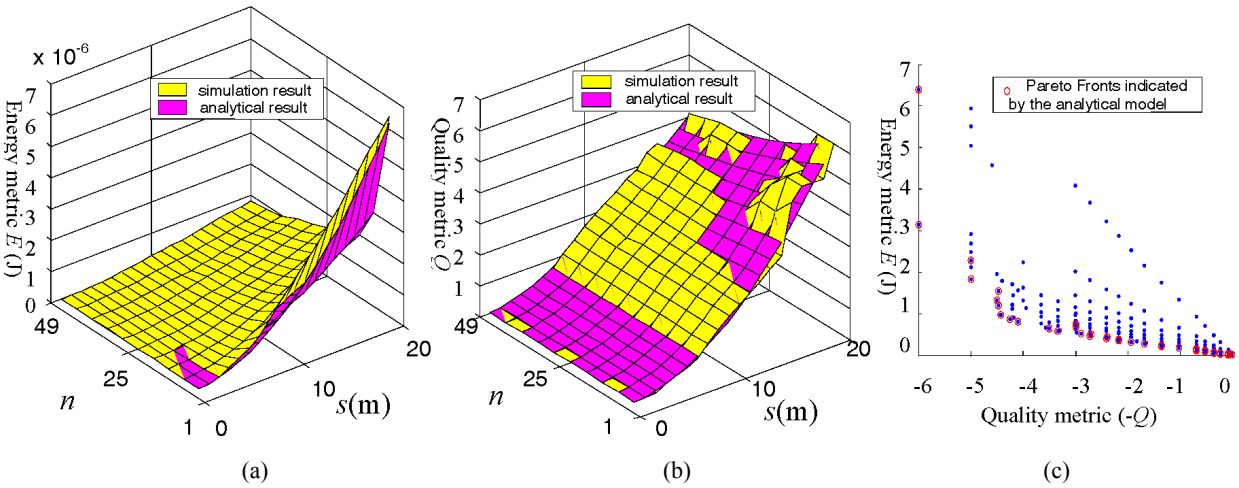

4.5 Verify the relationship in voronoi clusters

Can the relationship work in more general conditions? With this question, we verify its performance in voronoi clusters, which is the most popular in cluster-based tracking protocols (Chen et al., 2004). To construct voronoi clusters, CHs are generated 'Grid Uniformly' by Algorithm 1 and clusters are partitioned by the vonoroi diagram technique (Chen et al., 2004). Figure 13 shows an example of the topology of clusters for $n = 25$ and $N = 200$, where the clusters are in polygon shape.

In the target tracking scenario with non-overlapping clusters, the linear predictor is used to activate the downstream cluster. The target moves in the same typical trajectory. One hundred replications of simulations were run to evaluate the performances of every (n, s) pair. Analytical performance metrics are calculated with equations (9) and (10). When $N = 200$, $n = 25$, how the analytical Pareto Fronts perform in the simulations is plotted in Figure 14. Totally, 34 (n, s) pairs are found as the analytical Pareto Fronts from the relationship, and 28 of them are still Pareto

Fronts in the simulations. The coincident rate is 84.8%. More verification was done for different network settings and different target patterns. The results are summarised in Table 3. The coincident rates of Pareto Fronts provided by the relationship with uniformly hypothesised $f(x)$ are also shown. Although the coincident rate is reduced compared with those in the overlapping clusters, the worst case is still larger than 60%. They show that the relationship can still be adopted as an important design guideline for the selection of the cluster parameters even using non-overlapping clusters.

Table 2 Coincident rate of Pareto Fronts in different tracking scenarios

Target pattern	*Network setting*	*Coincident rate of Pareto fronts*	
		Normally hypothesised $f(x)$ (%)	*Uniformly hypothesised* $f(x)$ (%)
Linear motion, $v_x = 1$, $v_y = 1$	$N = 1000$	97.2	95.1
Linear in x and sine wave in y, $v_x = 2$, $v_y = 2$	$N = 200$	90.5	89.6
Directional random walk in x and random walk in y	$N = 200$	78.7	76.1

Figure 13 Non-overlapping cluster partition with vonoroi diagram (see online version for colours)

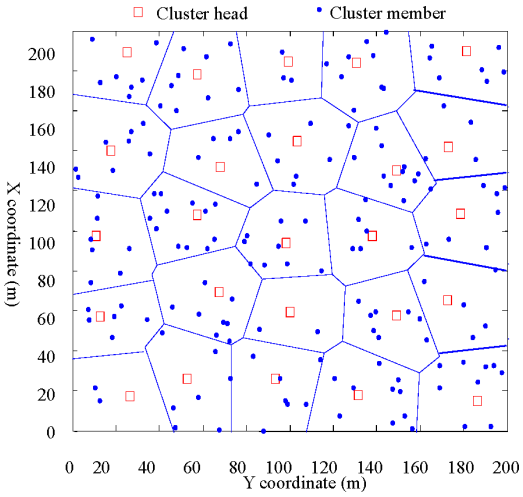

4.6 Discussion about the relationship effectiveness

We qualitatively analyse the reason for the high consistency between the analytical Pareto Fronts and the simulated Pareto Fronts. The main reason is due to the robustness of the order, which is an important concept in the ordinal optimisation (Ho, 1999). As shown in Figures 5 and 6, the quality metric and the energy metric are both monotone functions of n and s. The performance orders of the (n, s) pairs are more robust than their performance values, because small variation only changes their values but cannot change their orders. So that, even the conditions in the practical protocol are a little different from the ideal assumptions, the performance orders of the (n, s) pairs are easy to be kept. So that with either normally hypothesised $f(x)$ or uniformly hypothesised $f(x)$, the relationship can provide rather good Pareto fronts. These verifications validate the effectiveness of the derived relationship.

Figure 14 How the Pareto Fronts derived from the relationship perform in the simulation (see online version for colours)

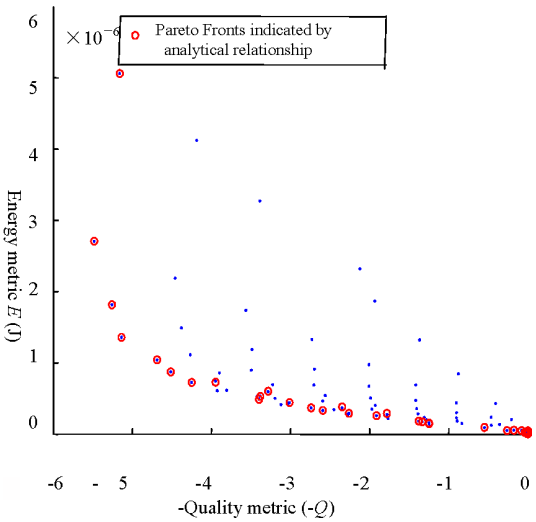

Table 3 Percent of coincident Pareto Fronts in different tracking scenarios

Target pattern	*Network setting*	*Coincident rate of Pareto fronts*	
		Normally hypothesised $f(x)$ (%)	*Uniformly hypothesised* $f(x)$ (%)
Linear motion, $v_x = 1$, $v_y = 1$	$N = 1000$	90.5	88.2
Linear in x and sine wave in y, $v_x = 2$, $v_y = 2$	$N = 200$	85.5	82.6
Directional random walk in x and random walk in y	$N = 200$	64.7	61.9

5 Related works

5.1 Wireless Sensor Network target tracking systems

WSN target tracking system has attracted great research attentions. In Demirbas et al. (2006), a sensor network system for vehicle tracking and autonomous interception was developed. In the system, an uncooperated agent called the evader runs freely, and an autonomous robot called pursuer is guided by a sensor network system to capture the evader. They studied the leader election, routing, network aggregation and closed loop control problems. In our previous work (Wang et al., 2006), we have developed a sensor network system for vehicle tracking. A test bed with 30 sensors was deployed in our campus to track the fast moving mobile bicycles to study the multiple target

tracking, dynamic clustering and routing. In Kwong et al. (2009), a cattle monitoring system using WSN was developed. The wireless sensors were used to continuously access the condition of the mobile individual animal, aggregating and reporting these data to the farm manager. Tracking position of the cattle is an important application in their system. In Wang et al. (2006), sensor networks were developed for farming application. In addition to the moisture sensor to monitor the soil condition, electronic tag readers, up to 40 sensors were used to track the cattle movements. Their sensors were solar powered and the test results of six months were reported. In Kwong et al. (2009), a sensor network system, called VigilNet, was developed to acquire and verify the information about enemy capabilities and positions of hostile targets. The middleware and integrated system of a network of 70 MICA2 motes were developed to track the positions of moving vehicles in an energy-efficient and stealthy manner. In Sikka et al. (2006), a virtual patrol system was developed to further improve the energy efficiency of the sensor network surveillance system. Coverage-based patrol and on-demand patrol were designed for energy-efficient node scheduling. Some other target tracking applications are summarised in He et al. (2006).

5.2 Node energy conserving and cluster schemes

As discussed in Kwong et al. (2009), Sikka et al. (2006) and He et al. (2006), energy efficiency is one of the most important requirements for the WSN tracking system. In Sharp et al. (2005) and Chen et al. (2004), it was reported that putting sensors into sleep mode could save energy up to three magnitudes, which is the most effective energy saving method compared to others (data aggregation, etc.). So with joint consideration of the distributed sensor organisation, cluster methods became a promising solution for energy-efficient sensor network design. LEACH (Heinzelman et al., 2000) proposed a hierarchical clustering scheme for information collection of sensor networks. By randomised cluster head erection and data aggregation, a factor of 7–8 improvement of the system lifetime was achieved compared with the non-clustering schemes. Our previous work proposed the energy-driven adaptive clusters (Wang et al., 2004) to solve the energy over-deplete problem of the cluster heads. It achieved a factor of 1–2.5 improvement of the system's lifetime than LEACH. In Younis and Fahmy (2004), hybrid energy-efficient distributed clustering was proposed to periodically select cluster heads according to a hybrid of the node residual energy and a secondary parameter, such as node proximity to its neighbours or node degree. It showed energy efficiency and scalability in data aggregation. PEGASIS (Lindsey and Raghavendra, 2002) proposed line-structure clusters, which achieved energy efficiency by hop by hop data aggregation. Geographical information of nodes was used in Xu and Heidemann (2001) to form the grid-based clusters and to activate the least number of nodes in each grid to meet the demand of communication. The neighbour coordination-based clustering scheme was proposed in SPAN (Chen et al., 2001), where only the required number of nodes was activated to assure the connectivity. Energy-aware management was proposed in Younis et al. (2003) to dynamically set routes and arbitrate medium access in the cluster to maximise the system's lifetime. These results focus on the energy efficiency of the cluster formation, which forms basics of the cluster-based target tracking protocols.

5.3 Cluster-based target tracking

The cluster-based target tracking protocols utilise the fact that only the sensors located in the vicinity of the mobile target can contribute to target detection. So they organise the sensors into dynamical clusters or static clusters, and do cluster-based sensor scheduling during target tracking. In DCTC (Zhang and Cao, 2004a), a dynamic convey tree-based collaboration scheme was proposed to dynamically construct a tree-structured cluster to track the target. The tree was rooted at the node closest to the target and was reconfigured when the distance from the target to the root exceeded a predetermined threshold. In Zhang and Cao (2004b), the tree reconfiguration problem was further formalised into a min-cost convey tree problem. In Chen et al. (2004), a cluster-based acoustic target tracking protocol was proposed. When an acoustic target moved in the sensing area, a cluster was dynamically constructed based on the captured acoustic energy of the sensors. This one-level cluster was dynamically reconfigured by the voronoi diagram method. Possible problems of these dynamical cluster-based tracking protocols are the frequent cluster reconfigurations, which may consume considerable amount of energy and may introduce overhead in tracking target. Static cluster is another approach. In Medeiros et al. (2008), for improving tracking accuracy and energy efficiency, distributed Kalman filter was developed in cluster-based target tracking in camera sensor networks. An adaptive distributed multi-sensor scheduling approach for target tracking in WSN was proposed in Lin et al. (2009). The optimal sampling interval for cluster activation is calculated. An energy-efficient prediction-based clustering algorithm is proposed in Deldar and Yaghmaee (2010) for optimising cluster activation. An ultrasound-based target tracking algorithm and its application in physical security are presented in Wang et al. (2009). A cluster partition and sensor network configuration algorithm are presented in Wang et al. (2005). A location-based vehicle movement prediction model for wireless communication is presented in Wu and Hsieh (2012). These cluster-based target tracking protocols were proposed almost with the same motivation that the cluster schemes can well trade-off between the energy efficiency and the tracking quality. A probabilistic model for studying the relationships of cluster-based fault tolerant target-tracking protocol was reported in Bhatti et al. (2012). However, such protocols have not quantitatively divided the underlying relationship between the clustering schemes and the system performances. The lack of deep understanding to this relationship leaves great difficulty for the tracking system design and optimisation.

6 Conclusion

In this paper, a novel convolution-based method is proposed to study the underlying relationship between the clustering schemes and the energy–quality performances of the cluster-based WSN tracking systems. This study is based on the fact that the various clustering schemes can be characterised by a set of cluster parameters, and the energy metric and the quality metric of the tracking systems are also dominated by these parameters. By proposing the number of contributable sensors as a novel quality metric, the relationship between tracking quality and cluster parameters was derived in closed form. With this result, how the cluster parameters affect the tracking system performances has been analysed, and the functions are used to optimise the design of the cluster-based tracking protocols by Pareto optimisation.

This derived relationship has been verified in an extensive manner in an OCT protocol and in a voronoi cluster-based tracking protocol. The result shows that the derived relationship can well predict the performances of the tracking protocol and can be used as a design to optimise the cluster parameters. The reason for the high effectiveness is also qualitatively discussed, which is mainly due to the robustness of the order.

Further study will focus on the network optimisation problem based on the performance constraints. More energy-efficient node scheduling, multiple channel access for fast-response target tracking, recovery scheme for target loss and dynamic cluster formation will be our future topics.

Acknowledgement

This work was supported by National Natural Science Foundation of China Grant Nos. 61073174, 61202360.

References

Aslam, J., Butler, Z., Constantin, F., Crespi, V., Cybenko, G. and Rus, D. (2003) 'Tracking a moving object with a binary sensor network', *Proceedings of SenSys'03: the First International Conference on Embedded Networked Sensor Systems*, Los Angeles, CA, USA, Association for Computing Machinery, New York, NY, USA, pp.150–161.

Bhatti, S. Memon, S. Jokhio, I.A. and Memon, M.A. (2012) 'Modelling and symmetry reduction of a target-tracking protocol using wireless sensor networks', *IET Communications*, Vol. 6, No. 10, p.1205.

Chen, B., Jamieson, K., Balakrishnan, H. and Morris, R. (2001) 'Span: an energy-efficient coordination algorithm for topology maintenance in ad hoc wireless networks', *Proceedings of the 6th ACM MOBICOM Conference*, Rome, pp.481–491.

Chen, W.P., Hou, J.C. and Sha, L. (2004) 'Dynamic clustering for acoustic target tracking in wireless sensor networks', *IEEE Transactions on Mobile Computing*, Vol. 3, No. 3, pp.258–271.

Deldar, F. and Yaghmaee, M.H. (2010) 'Energy efficient prediction-based clustering algorithm for target tracking in wireless sensor networks', *2nd International Conference on Intelligent Networking and Collaborative Systems (INCOS)*, Thessaloniki, Greece, pp.315–318.

Demirbas, M., Chow, K.Y. and Wan, C.S. (2006) 'INSIGHT: internet-sensor integration for habitat monitoring', *Proceedings of the 2006 International Symposium on World of Wireless, Mobile and Multimedia Networks*, Washington DC, USA, pp.553–558.

He, T., Vicaire, P., Yan, T., Luo, L., Gu, L., Zhou, G., Stoleru, R., Cao, Q., Stankovic, J.A. and Abdelzaher, T. (2006) 'Achieving real-time target tracking using wireless sensor networks', *In IEEE RTAS 2006*, Washington, DC, USA, pp.33–48.

Heinzelman, W.R., Chandrakasan, A. and Balakrishnan, H. (2000) 'Energy-efficient communication protocol for wireless microsensor networks', *Proceedings of The Hawaii International Conference on System Sciences*, Maui, USA, IEEE, Los Alamitos, CA, USA, p.223.

Ho, Y.C. (1999) 'An explanation of ordinal optimization: soft computing for hard problems', *Information Sciences*, Vol. 113, Nos. 3–4, pp.169–192.

Kwong, K.H., Wu, T.T., Goh, H.G., Stephen, B., Gilroy, M., Michie, C. and Andonovic, I. (2009) 'Wireless sensor networks in agriculture: cattle monitoring for farming industries', *PIERS Online*, Vol. 5, No. 1, pp.31–35.

Lin, J., Xiao, W., Lewis, F.L. and Xie, L. (2009) 'Energy-efficient distributed adaptive multisensor scheduling for target tracking in wireless sensor networks', *IEEE Transactions on Instrumentation and Measurement*, Vol. 58, No. 6, June, pp.1886–1896.

Lindsey, S. and Raghavendra, C. (2002) 'PEGASIS: power-efficient gathering in sensor information systems', *Proceedings of IEEE Aerospace Conference*, pp.1125–1130.

Medeiros, H., Park, J. and Kak, A. (2008) 'Distributed object tracking using a cluster-based kalman filter in wireless camera networks', *IEEE Journal of Selected Topics in Signal Processing*, Vol. 2, No. 4, August, pp.448–463.

Priyantha, N.B., Chakraborty, A. and Balakrishnan, H. (2000) 'Cricket location-support system', *Proceedings of the Annual International Conference on Mobile Computing and Networking, MOBICOM*, Boston, MA, USA, ACM, New York, NY, USA, pp.32–43.

Sharp, C., Schaffert, S., Woo, A., Sastry, N., Karlof, C., Sastry, S. and Culler, D.E. (2005) *Proc. EWSN*, pp.93–107.

Sikka, P., Corke, P., Valencia, P., Crossman, C., Swain, D. and Bishop-Hurley, G. (2006) 'Wireless ad hoc sensor and actuator networks on the farm', *IPSN'06*, New York, NY, USA, pp.492–499.

Wang, X., Ma, J., Wang, S. and Bi, D. (2010) 'Distributed energy optimization for target tracking in wireless sensor networks', *IEEE Transactions on Mobile Computing*, Vol. 9, No. 1, January, pp.73–86.

Wang, Y., Han, D., Zhao, Q., Guan, X. and Zheng, D. (2005) 'Clusters partition and sensors configuration for target tracking in wireless sensor networks', in Wu, Z., Chen, C., Guo, M. and Bu, J. (Eds.): *Embedded Software and Systems*, Vol. 3605, Springer Berlin/Heidelberg, pp.333–338.

Wang, Y., Zhao, J. and Fukushima, T. (2009) 'LOCK: a highly accurate, easy-to-use location-based access control system', in Choudhury, T., Quigley, A., Strang, T. and Suginuma, K. (Eds.): *Location and Context Awareness*, Vol. 5561, Springer Berlin/Heidelberg, pp.254–270.

Wang, Y., Zhao, Q. and Zheng, D. (2004) 'Energy-driven adaptive clustering data collection protocol in wireless sensor networks', *Proceedings of International Conference on Intelligent Mechatronics and Automation*, Chengdu, China, pp.599–604.

Wang, Y., Wang, C., Tang, W., Zhao, Q., Zheng, D. and Guan, X. (2006) 'A vehicle tracking system based on wireless sensor network', *Information and Control*, Vol. 35, No. 2, pp.169–178.

Wu, H.T. and Hsieh, W.S. (2012) 'Location-based vehicular moving predictions for wireless communication', *International Journal of Ad Hoc and Ubiquitous Computing*, Vol. 10, No. 4, p.197.

Xu, Y. and Heidemann, J. (2001) 'Geography-informed energy conservation for ad hoc routing', *Proceedings of IEEE/ACM MobiCom*, Rome, Italy, pp.16–21.

Younis, M., Youssef, M. and Arisha, K. (2003) 'Energy-aware management for cluster-based sensor networks', *Computer Networks-the International Journal of Computer and Telecommunications Networking*, Vol. 43, No. 5, pp.649–668.

Younis, O. and Fahmy, S. (2004) 'HEED: a hybrid, energy-efficient, distributed clustering approach for ad hoc sensor networks', *IEEE Transactions on Mobile Computing*, Vol. 3, No. 4, December, pp.366–379.

Zhang, W. and Cao, G. (2004b) 'Optimizing tree reconfiguration for mobile target tracking in sensor networks', *Proceedings of IEEE INFOCOM 2004,Twenty-Third Annual Joint Conference of the IEEE Computer and Communications Societies*, Hong Kong, China, Institute of Electrical and Electronics Engineers Inc., Piscataway, NJ, USA, pp.2434–2445.

Zhang, W.S. and Cao, G.H. (2004a) 'DCTC: Dynamic convoy tree-based collaboration for target tracking in sensor networks', *IEEE Transactions on Wireless Communications*, Vol. 3, No. 5, pp.1689–1701.

Appendix

In the first kind of detection schemes, each contributable sensor can give an independent estimation to the target's position. Suppose the number of the contributable sensors is n and the n_s estimations are $\{\hat{\boldsymbol{\theta}}_1, \hat{\boldsymbol{\theta}}_2, ..., \hat{\boldsymbol{\theta}}_{n_s}\}$ with Gaussian white noise. Denote the estimated position of the target as $\hat{\boldsymbol{\theta}}$. With estimation theory, we have

$$\mathrm{var}(\hat{\boldsymbol{\theta}}) = \frac{1}{n_s}\sum_{n=1}^{n_s}\mathrm{var}(\hat{\boldsymbol{\theta}}_i).$$

The estimation variance is of magnitude $O(1/\sqrt{n_s})$.

- In the second kind of schemes, the estimation variance can also be proved in the magnitude of $O(1/\sqrt{n_s})$. The position of target can be determined by at least three contributable sensors. Suppose the coordinates of these sensors are (x_1, y_1), (x_2, y_2), (x_3, y_3), respectively, and they are not on the same line. We denote the actual position of the target as (x_a, y_a) and denote its estimated position as (x_e, y_e). For every sensor, its measured distance to the target is denoted by $\hat{d}_i$. where $i = 1, 2, 3$ is the number of sensors. If the variance of the measured distance is σ_d, the actual position of the target should be located within a ring around the sensor, with mean distance $\hat{d}_i$ and variance σ_d. Let α_i denote the angle from the x-axis to the line $y = y_i x / x_i$ ($i = 1, 2, 3$). As the real position of the target is within the overlapping area of the three rings, the variance of the estimated position is bounded by

$$\sigma_x \le \sigma_d \cos\alpha_1 + \sigma_d \cos\alpha_2 + \sigma_d \cos\alpha_3 \le 3\sigma_d,$$
$$\sigma_y \le \sigma_d \sin\alpha_1 + \sigma_d \sin\alpha_2 + \sigma_d \sin\alpha_3 \le 3\sigma_d,$$

where σ_x and σ_y are the variances of the estimation in the x and y directions. We denote σ as the variance of the estimated position, then even in the worst case, it is bounded as $\sigma \le 3\sqrt{2}\sigma_d$. So that the variance of the estimation is of magnitude $O(1/\sqrt{n_s/3\sqrt{2}})$, which is also $O(1/\sqrt{n_s})$.

- In the third kind of schemes, locations of the sensors are used as the independent observations of the target's position in the centroid method. If n_s contributable nodes are within the target-detectable region, similarly like in the first scheme, the variance of the estimation is of magnitude $O(1/\sqrt{n_s})$. The difference between this scheme and the first scheme is that in order to improve the estimation accuracy, this scheme has to increase the node density, while the first scheme can only increase the frequency of the observations.